

000 001 002 003 004 005 BENCHDEPTH: ARE WE ON THE RIGHT WAY TO 006 EVALUATE DEPTH FOUNDATION MODELS? 007 008 009

010 **Anonymous authors**
011 Paper under double-blind review
012
013
014
015
016
017
018
019
020
021
022
023
024
025
026
027
028
029
030
031
032
033
034
035
036
037
038
039
040
041
042
043
044
045
046
047
048
049
050
051
052
053

ABSTRACT

Depth estimation is a fundamental task in computer vision with diverse applications. Recent advancements in deep learning have led to powerful depth foundation models (DFMs), yet their evaluation remains focused merely on geometry accuracy. Given the fact that downstream tasks increasingly rely on depth as guidance, we present **BenchDepth**, a new benchmark that evaluates DFMs through five carefully selected proxy tasks: depth completion, stereo matching, monocular feed-forward 3D scene reconstruction, SLAM, and vision-language spatial understanding. Our approach assesses DFMs based on their practical utility in real-world applications and provides complementary information to traditional benchmarks. We benchmark **eight** state-of-the-art DFMs and provide an in-depth analysis of key findings and observations. Interestingly, our results reveal discrepancies between rankings on traditional geometric benchmarks and those on downstream tasks, suggesting that existing evaluation protocols do not fully capture the practical effectiveness of DFMs. This underscores the importance of BenchDepth as a complementary benchmark, bridging the gap between geometry-centric metrics and application-driven evaluation.

1 INTRODUCTION

Depth estimation plays a crucial role in various computer vision applications, from 3D scene reconstruction, autonomous driving, to robotics Zhang et al. (2023); Li et al. (2023b); Zhu et al. (2024); Szymanowicz et al. (2024). In recent years, deep learning-based approaches have significantly advanced the field, leading to powerful foundation models capable of generating high-quality depth predictions across diverse input domains Eigen et al. (2014); Bhat et al. (2023); Ke et al. (2024); Yang et al. (2024b); Ranftl et al. (2022); Wang et al. (2024a; 2025). However, despite these advancements, evaluating and comparing depth estimation models remains an open challenge Ge et al. (2024). Existing evaluation protocols primarily emphasize geometry accuracy, which does not necessarily reflect the utility of depth in real-world applications.

Meanwhile, downstream tasks increasingly rely on depth as guidance, emphasizing the need for an evaluation framework that can reveal a model’s potential across various applications Park et al. (2024); Szymanowicz et al. (2024); Zhu et al. (2024); Jiang et al. (2025); Cheng et al. (2025). Traditional benchmarks focus on constrained numerical accuracy, overlooking how different models generalize when deployed in application-driven tasks Ge et al. (2024). This disconnect often leads to discrepancies: models that excel in geometric benchmarks may not perform as well when integrated into end-to-end frameworks for practical applications.

To address this gap, we propose a new approach for benchmarking depth foundation models. Rather than relying solely on traditional depth evaluation metrics, we use downstream tasks as proxy tasks for model evaluation. By design, our benchmark shifts the focus from numerical alignment-based metrics to application-driven performance, thereby providing a complementary perspective on model capability. This direction is inspired by the success of large language models (LLMs), vision language models (VLMs), and self-supervised learning methods Achiam et al. (2023); Li et al. (2023a); He et al. (2020); Oquab et al. (2023); Siméoni et al. (2025), where the evaluation is often based on downstream tasks.

To this end, we propose **BenchDepth**, a benchmark consisting of five downstream proxy tasks: stereo matching Xu et al. (2023), depth completion Park et al. (2024), monocular feed-forward

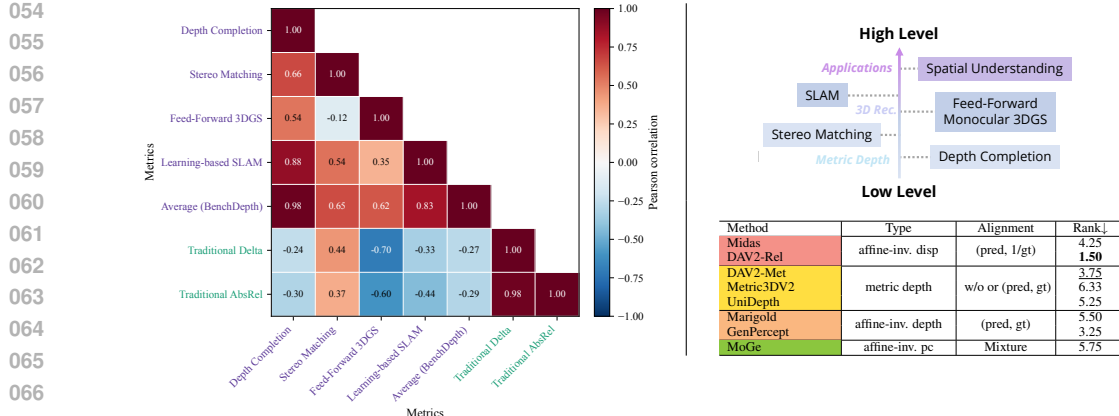


Figure 1: **BenchDepth** illustration, results, and comparison with traditional benchmarks. **Left:** Pearson correlation matrix between **BenchDepth** and the **standard benchmark** results. Proxy tasks exhibit strong internal consistency, indicating that **BenchDepth** captures meaningful shared structure across tasks and has the potential to generalize to other proxy tasks. Moreover, correlations between **BenchDepth** and traditional benchmarks are generally weaker or even negative, underscoring the gap between geometry-centric metrics and downstream utility. **Right:** We evaluate different types of depth predictions (highlighted with different colors) with proxy tasks in a bottom-to-top manner. We show the average rank of each depth method in the bottom right table. Different methods utilize different alignment strategies on the traditional benchmark, which is not necessary on **BenchDepth**.

3D scene reconstruction Szymanowicz et al. (2024), SLAM Zhu et al. (2024), and 3D-VQA Zuo et al. (2024). The tasks are selected in a bottom-to-top manner as shown in Fig. 1, ranging from applications in low-level to high-level vision. *Our goal is not to replace traditional metrics, but to complement them by revealing their limitations and proposing an application-driven benchmark that better reflects how DFM are used in practice.*

In this paper, we benchmark **eight** state-of-the-art 3D foundation models with DepthBench. By examining their performance across proxy tasks, we provide new insights into what constitutes a good foundation depth model. **Notably**, our results reveal **discrepancies between rankings on traditional geometric benchmarks** Ge et al. (2024); Wang et al. (2024a) (We refer to the original papers for details about standard benchmark ranking) **and those on downstream tasks**, indicating that existing evaluation protocols do not fully capture the practical effectiveness of DFM. Our main findings and conclusions are as follows:

1. Our correlation analysis (Fig. 1) shows stronger consistency among proxy tasks (e.g., depth completion and SLAM: 0.88), indicating that the selected five tasks collectively form a representative and coherent benchmark. At the same time, correlations with traditional metrics are weaker or even negative, further emphasizing the gap between geometry-based evaluation and real-world utility.
2. Most depth foundation models improve the performance of downstream tasks, highlighting their potential for broader applications in the future.
3. Overall, DAV2 Yang et al. (2024b) achieves the best results across proxy tasks, demonstrating the benefits of scaling up training data and incorporating synthetic data.
4. Affine-invariant disparity methods consistently outperform other depth estimation approaches, even with MiDaS Ranftl et al. (2022) being the oldest method among them.
5. Despite being fine-tuned on a single dataset (Hypersim Roberts et al. (2021), synthetic), DAV2-Met significantly outperforms other metric depth models Hu et al. (2024); Piccinelli et al. (2024) trained on multiple datasets. This aligns with the conclusion of ZoeDepth Bhat et al. (2023) that fine-tuning a well-pretrained affine-invariant disparity model enhances metric depth estimation. Moreover, the performance gap suggests that incorporating synthetic data for metric depth training is crucial, as it allows models to learn high-frequency details that are often lost in real-world datasets Yang et al. (2024b); Li et al. (2024).

108 6. The performance improvement from Marigold Ke et al. (2024) to GenPercept Xu et al.
 109 (2024) underscores the importance of effective fine-tuning strategies for Stable Diffusion
 110 Rombach et al. (2022), a powerful foundation model. Expanding the training data
 111 could further unlock their potential, following the success of other methods, as the current
 112 fine-tuning process is limited to VKITTI Geiger et al. (2013) and Hypersim.
 113 7. MoGe Wang et al. (2024a), as a novel approach for geometry estimation, demonstrates
 114 potential on DepthBench, though further research is needed to improve its performance.
 115 8. For the highest-level task, VLM spatial understanding, all methods yield comparable re-
 116 sults. This suggests that at this higher level, different depth estimation approaches can be
 117 equally effective.
 118

119 We hope that our work will spark further discussion in the community about the best practices for
 120 depth model evaluation and pave the way for further research and development of depth estimation.
 121

122 2 RELATED WORKS

124 2.1 DEPTH FOUNDATION MODEL (DFM)

126 Monocular depth estimation has seen significant advancements with the availability of large-scale
 127 public datasets Silberman et al. (2012); Geiger et al. (2012); Cordts et al. (2016), improved archi-
 128 tectural designs Eigen et al. (2014); Li et al. (2023d); Bhat et al. (2021); Li et al. (2023c), and
 129 enhanced training strategies Chen et al. (2016); Fu et al. (2018); Li et al. (2022), *etc.* While earlier
 130 works primarily focused on achieving high performance in in-domain inference, the scaling of both
 131 models and datasets in deep learning Kaplan et al. (2020) has shifted recent research toward devel-
 132 oping foundation models with strong zero-shot generalization across unseen domains (*i.e.*, diverse
 133 real-world images).

134 For example, MiDaS Ranftl et al. (2022) introduces a mixture-dataset training approach and adopts
 135 an affine-invariant disparity representation to handle cross-dataset inconsistencies. DAV2 Yang et al.
 136 (2024a;b) follows a similar formulation but scaled training further using a semi-supervised learning
 137 paradigm. Other works leverage the prior knowledge of Stable Diffusion Rombach et al. (2022) and
 138 fine-tune pretrained models for affine-invariant depth estimation Ke et al. (2024); Xu et al. (2024).
 139 Other lines of research such as Metric3DV2 Hu et al. (2024) and UniDepth Piccinelli et al. (2024)
 140 aim to predict metric depth by incorporating explicit camera models. MoGe Wang et al. (2024a) pro-
 141 poses a novel formulation using affine-invariant point maps Wang et al. (2024b) to represent monocu-
 142 lar geometry. Despite the rapid progress in depth foundation models, a key challenge remains: how
 143 to evaluate and compare these models in a way that meaningfully reflects their effectiveness across
 144 diverse real-world applications.
 145

146 2.2 EVALUATIONS OF DFMs

147 Eigen *et al* Eigen et al. (2014) introduced the first deep learning framework for monocular *metric*
 148 depth estimation, along with several standard evaluation metrics that remain widely used today.
 149 However, while depth estimation methods have diversified into various depth representations (as
 150 summarized in Tab. 1), existing works attempt to adopt the same evaluation protocol designed for
 151 metric depth estimation Ranftl et al. (2022); Yang et al. (2024b); Hu et al. (2024); Ke et al. (2024);
 152 Xu et al. (2024); Wang et al. (2024a).
 153

In contrast, recent progress in other domains such as large language models (LLMs), vision-language
 154 models (VLMs), and self-supervised learning methods Achiam et al. (2023); Li et al. (2023a);
 155 He et al. (2020); Oquab et al. (2023); Siméoni et al. (2025)—demonstrates the importance of
 156 downstream-task evaluation for revealing the true potential of foundation models. Inspired by this,
 157 we propose an application-driven benchmark that assesses DFMs through five carefully selected
 158 proxy tasks, ranging from low-level to high-level vision.
 159

160 Compared with previous benchmarks such as E3D-Bench Cong et al. (2025), which emphasizes
 161 multi-view geometry, and GeoBench Ge et al. (2024), which focuses on monocular depth estima-
 162 tion with traditional metrics, our benchmark shifts the emphasis toward downstream applications.
 163 By focusing on the monocular setting and evaluating depth estimation through real-world tasks,
 164

162 BenchDepth provides a complementary perspective to geometry-centric evaluation and contributes
 163 to a more holistic understanding of depth foundation models.
 164

166 3 BENCHDEPTH

168 We introduce **BenchDepth**, a novel benchmark for depth estimation based on carefully selected
 169 proxy tasks in a bottom-up manner (Fig. 1). Our design philosophy is to span a wide range of
 170 applications, from low-level tasks closely tied to depth prediction to high-level tasks where depth
 171 provides auxiliary guidance. This ensures that the evaluation reflects the practical utility of DFM
 172 across diverse downstream scenarios.

174 3.1 TASK SELECTION

176 We group the proxy tasks into three levels:

177 **Low-level tasks: depth completion and stereo matching.** These tasks are closely related to metric
 178 depth estimation and differ mainly in their input prompts—sparse depth from sensors or stereo pairs
 179 with a fixed baseline. While the methods include task-specific components, we keep the architecture,
 180 training pipeline, and datasets strictly fixed across all experiments. The only variable is the input
 181 depth map from each DFM. As a result, performance differences serve as a fair and informative
 182 evaluation signal of the practical effectiveness of DFM.

183 **Mid-level tasks: feed-forward 3D Gaussian Splatting (3DGS) and SLAM.** These tasks require
 184 more complex 3D reconstruction and differ in both representation (Gaussian splats vs. neural
 185 implicit) and input regime (single-view vs. multi-view), broadening the scope of our benchmark. Al-
 186 though less directly tied to DFM than low-level tasks, recent studies have shown the growing use of
 187 DFM predictions as priors in these domains Szymanowicz et al. (2024); Zhu et al. (2024). By align-
 188 ing architectures, training setups, and datasets, we ensure that observed performance differences can
 189 be attributed solely to the depth predictions of DFM.

190 **High-level task: vision-language spatial understanding.** At the highest level, we evaluate the
 191 contribution of DFM to VLMs Cai et al. (2024), where depth serves as a geometric prior for rea-
 192 soning about 3D spatial relations. While performance differences are less pronounced here, the
 193 results reveal an important limitation: *current VLMs tend to rely on coarse layout cues, showing*
 194 *limited sensitivity to fine-grained depth errors.* Including this task highlights both the opportunities
 195 and the challenges of integrating depth into semantic reasoning systems, pointing to future research
 196 directions.

197 Together, these five tasks span different levels of abstraction, allowing users to focus on the evalua-
 198 tions most relevant to their applications.

200 3.2 MODEL SELECTION

202 Selected depth foundation estimation methods for benchmarking are summarized in Tab. 1. We
 203 choose the most representative methods from each depth estimation category. Note that though
 204 DAV2-Met Yang et al. (2024b), Metric3DV2 Hu et al. (2024), and UniDepth Piccinelli et al. (2024)
 205 are all metric methods, DAV2-Met is fine-tuned on a single metric dataset (Hypersim Roberts et al.
 206 (2021)), whereas the other two methods are trained with a mixture of many datasets. We use the
 207 default camera parameter assumption for Metric3DV2 and UniDepth. Since the original version of
 208 Marigold Ke et al. (2024) is hard to adapt to online training due to the large number of inference
 209 steps, we use the end-to-end fine-tuned version of Marigold Garcia et al. (2024) that supports one-
 210 step inference as a replacement.

211 For each proxy task, we use recent and well-integrated baselines selected for their compatibility with
 212 external depth inputs and representation diversity. DepthPrompting Park et al. (2024), Flash3D Szy-
 213 manowicz et al. (2024), NICER-SLAM Zhu et al. (2024), and SpatialBot Cai et al. (2024) are all
 214 representative methods that explicitly incorporate DFM in their design. IGEV Xu et al. (2023)
 215 does not use DFM directly but serves as an important baseline for subsequent DFM-integrated
 stereo models such as FoundationStereo Wen et al. (2025) and DEFOM-Stereo Jiang et al. (2025).

216 **Table 1: Benchmark with metric depth completion.** We select DepthPrompting Park et al. (2024)
 217 as the baseline method and apply depth predictions from various foundation models as the guidance.
 218 We use different amounts of sparse samples (from 100 to 1) in this experiment. Best results are in
 219 **bold**, second best are underlined. *imp.* (%) indicates the average improvement ratio, and *rank* is
 220 calculated based on it. w/o depth refers to the baseline with only GT sparse depth as guidance.

Method	100		32		8		4		1		<i>imp.</i>	<i>rank</i>
	RMSE	MAE										
w/o depth	0.206	<u>0.102</u>	0.334	0.199	0.486	0.340	0.514	0.370	0.550	0.406	-	-
Midas	0.204	0.114	0.294	0.182	0.449	0.311	0.493	0.355	0.556	0.414	+3.09	4
DAV2-Rel	0.191	0.099	<u>0.279</u>	0.166	<u>0.427</u>	0.292	0.471	0.336	<u>0.533</u>	<u>0.396</u>	+9.26	1
DAV2-Met	0.202	0.112	0.287	0.178	<u>0.431</u>	<u>0.297</u>	0.472	<u>0.338</u>	0.529	0.392	+6.48	2
Metric3DV2	0.216	0.128	0.306	0.195	0.454	0.317	0.497	0.359	0.557	0.415	-0.38	8
UniDepth	0.210	0.122	0.296	0.187	0.438	0.308	0.480	0.349	0.540	0.404	+2.97	5
Marigold	0.210	0.121	0.296	0.187	0.448	0.314	0.491	0.356	0.555	0.414	+1.76	6
GenPercept	0.199	0.110	<u>0.284</u>	<u>0.174</u>	0.436	0.301	0.479	0.342	0.542	0.402	+6.16	3
MoGe	0.210	0.124	0.295	0.188	0.444	0.312	0.489	0.355	0.558	0.417	+1.53	7

232 Most importantly, all selected baselines provide official training code, and our benchmark is directly
 233 developed on top of their implementations. More details are presented in Sec. 3.4.

234 When developing BenchDepth, we intentionally fix all aspects of the downstream pipeline. We
 235 either follow the default integration strategy used in the original papers or apply the most straight-
 236 forward approach Zhang et al. (2023); Xu et al. (2023). Importantly, we restrict evaluation to the
 237 *predicted depth maps* from DFM, excluding intermediate features. This avoids unfair advantages
 238 from model-specific backbones and ensures that the only factor varying across experiments is the
 239 DFM output. Although DFM are not explicitly optimized for these tasks, the consistent perfor-
 240 mance differences observed validate BenchDepth as a fair measure of their relative effectiveness.

241 3.3 SCALABILITY

242 We acknowledge that downstream performance can also depend on the choice of the task archi-
 243 tecture. In this work, we evaluate one representative model per task. While this design provides
 244 a controlled comparison and keeps the benchmark tractable, we view BenchDepth as a *framework*
 245 rather than a fixed set of results. Future work could include additional architectures, tasks such as
 246 video depth estimation or surface reconstruction, and stronger baselines (*e.g.*, 3DGS-based SLAM).

247 Our evaluation metrics are reported per task, reflecting the standards commonly used in each domain
 248 (*e.g.*, EPE for stereo, PSNR for view synthesis). To provide a broader perspective, we also compute
 249 improvement-over-baseline percentages and average rankings across tasks (Fig. 1).

250 In addition, we conduct a correlation study between BenchDepth results and traditional benchmarks.
 251 Specifically, we compute the Pearson correlation matrix between the average improvement on our
 252 proxy tasks and the standard benchmark results. The analysis (Fig. 1) reveals two key observations:
 253 (1) proxy tasks exhibit strong internal consistency, with depth completion and SLAM showing a par-
 254 ticularly high correlation (0.88), indicating that our benchmark captures meaningful shared structure
 255 across tasks and has the potential to generalize to other proxy tasks; (2) correlations between proxy
 256 tasks and traditional benchmarks are generally weak and even negative, underscoring the gap be-
 257 tween geometry-centric metrics and downstream utility. More details about this correlation study
 258 are presented in Sec. 4.

259 BenchDepth thus establishes a starting point for application-driven evaluation of DFM. While
 260 not exhaustive, it demonstrates that DFM have measurable and consistent impacts across diverse
 261 downstream settings, and highlights both their strengths and limitations when applied in practice.

262 3.4 DETAILS

263 Below, we present the five proxy tasks in detail and describe the modifications applied to selected
 264 methods to support depth evaluation using DepthBench. We use 8 GPUs to conduct the benchmark.

265 **Depth Completion:** Given sparse metric-scale depth measurements from sensors (*e.g.* LiDAR,
 266 Radar) and corresponding images, depth completion aims to generate dense metric depth predic-

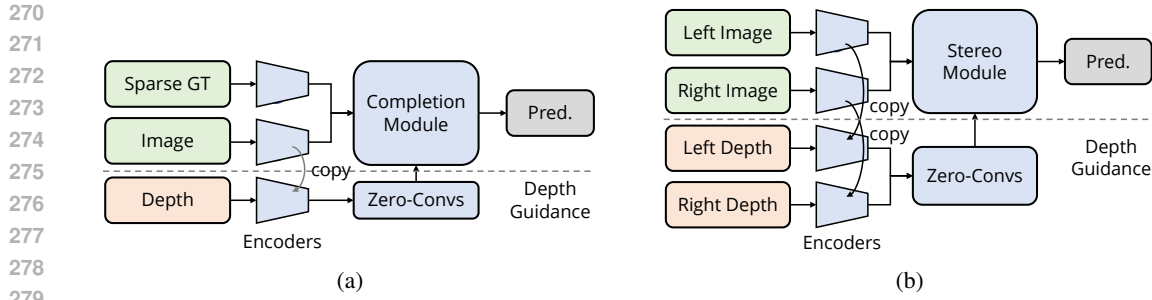


Figure 2: **(a)** Depth completion framework and **(b)** Stereo matching framework for depth benchmark. We adopt zero convolutions Zhang et al. (2023) to introduce depth guidance without modifying core components of proxy tasks.

We select DepthPrompting Park et al. (2024) as the baseline method. While DepthPrompting enables the adaptation of foundation depth models for completion, its reliance on feature extractors from these models Li et al. (2023d) introduces bias, as the extractor quality may influence performance more than the predicted depth itself. To mitigate this, we standardize feature extractors across models and inject depth predictions using zero convolutions Zhang et al. (2023) (Fig. 2a). Additionally, we omit the alignment module in DepthPrompting to enable direct comparisons across depth methods. We use the NYU Depth V2 dataset Silberman et al. (2012) for this proxy task, following the official split with about 50k training samples and 654 testing samples.

Stereo Matching: This task estimates disparity from two images with a known baseline. Metric depth can be recovered from disparity using camera parameters. We adopt IGEV Xu et al. (2023) as our baseline and incorporate zero convolutions Zhang et al. (2023) to inject depth predictions as shown in Fig. 2b. Unlike prior works that develop task-specific strategies to integrate depth into stereo matching models Cheng et al. (2025); Jiang et al. (2025), our simple yet general approach allows for a more straightforward assessment of depth prediction quality. We use the SceneFlow dataset Mayer et al. (2016), which contains 35,454 training pairs and 4,370 test pairs with dense disparity maps. Middlebury 2014 Scharstein et al. (2014) and ETH3D Schops et al. (2017) are used for zero-shot evaluation.

Feed-Forward Monocular 3DGS: This task reconstructs scenes and synthesizes novel views from a single image using 3D Gaussian Splatting Kerbl et al. (2023). We use Flash3D Szymanowicz et al. (2024) as the baseline model. Flash3D incorporates a frozen depth foundation model in its first stage to estimate depth from the input image. The predicted depth and image are then processed by a UNet-like Ronneberger et al. (2015) network to estimate 3DGS parameters. Since the foundation depth model remains frozen and no features from the foundation model are used in the second stage, we can adopt different foundation models for the first stage and train Flash3D following the default recipe. We use the RealEstate10k dataset Zhou et al. (2018). It consists of real estate videos from YouTube, with 67,477 training scenes and 7,289 test scenes. Some outdated samples were removed, causing slight deviations from the results reported in Szymanowicz et al. (2024). The baseline result is obtained by directly using the officially released model with unmodified code.

Simultaneous Localization and Mapping: Simultaneous Localization and Mapping (SLAM) is a fundamental problem in computer vision with broad applications. We employ NICER-SLAM Zhu et al. (2024) as our baseline, as it integrates dense SLAM with a neural implicit representation for tracking and mapping from monocular RGB videos. Since NICER-SLAM can process RGB-D sequences, we replace the original sensor depth with depth predictions from different foundation models and train the system accordingly. To better assess the impact of depth predictions, we omit pseudo-depth loss during training. We evaluate models on the Replica dataset Straub et al. (2019), which provides RGB-(D) images rendered using the official renderer. All 8 scenes are used for benchmarking. For benchmarking, we replace the original input depth with estimated depth from different methods and omit the monocular depth loss (Eq. 13 in Zhu et al. (2024)), which depends on another depth model. We exclude Metric3DV2 since it was trained on this dataset, though there is no evidence of overfitting.

324 Table 2: **Benchmark with stereo matching.** We select IGEV Xu et al. (2023) as the baseline
 325 method and apply depth predictions from various foundation models as the guidance to fine-tune the
 326 baseline model.

Method	SceneFlow		Middlebury		ETH3D		<i>imp.</i>	<i>rank</i>
	EPE \downarrow	>3pt(%) \downarrow	EPE \downarrow	>2pt(%) \downarrow	EPE \downarrow	>1pt(%) \downarrow		
w/o depth	0.496	2.599	0.857	6.655	0.283	3.575	-	-
Midas	0.483	2.502	1.061	7.316	0.273	3.383	-3.07	7
DAV2-Rel	0.456	2.432	0.834	6.399	0.275	3.189	+5.77	1
DAV2-Met	0.471	2.473	0.938	6.177	0.270	3.698	+1.46	5
Metric3DV2	0.482	2.521	0.949	7.309	0.275	3.523	-1.74	6
UniDepth	0.477	2.521	0.964	7.242	0.285	3.822	-3.68	8
Marigold	0.475	2.499	0.899	6.519	0.273	3.485	+1.87	4
GenPercept	0.473	2.485	0.935	6.649	0.265	<u>3.374</u>	+1.99	3
MoGe	0.473	2.481	0.907	5.951	0.279	3.544	<u>+2.70</u>	2

337 Table 3: **Benchmark with feed-forward monocular 3D scene reconstruction by novel view synthesis.** We select Flash3D Szymanowicz et al. (2024) as the baseline method and apply depth pre-
 338 dictions from various foundation models as the model input. Following Szymanowicz et al. (2024), we present results of small, medium and large baseline ranges separately.

Method	5 frames			10 frames			$\mathcal{U}[-30, 30]$ frames			<i>imp</i>	<i>rank</i>
	PSNR \uparrow	SSIM \uparrow	LPIP \downarrow	PSNR \uparrow	SSIM \uparrow	LPIP \downarrow	PSNR \uparrow	SSIM \uparrow	LPIP \downarrow		
w/o depth	24.285	0.803	0.151	21.767	0.729	0.203	21.241	0.705	0.230		
Midas	24.964	0.812	0.125	22.290	0.735	0.179	21.769	0.710	0.212	+5.24	1
DAV2-Rel	24.965	0.812	0.129	22.305	0.733	0.185	21.703	0.706	0.218	+4.21	3
DAV2-Met	25.000	0.812	0.128	22.341	0.735	0.182	21.842	0.711	0.215	+4.81	2
Metric3DV2	24.468	0.787	0.150	21.994	0.713	0.204	21.396	0.690	0.233	-0.05	5
UniDepth	23.983	0.786	0.145	21.530	0.708	0.202	21.036	0.687	0.235	-0.10	6
Marigold	23.974	0.779	0.162	21.515	0.701	0.219	20.952	0.676	0.248	-4.19	8
GenPercept	24.119	0.787	0.140	21.489	0.705	0.197	21.029	0.682	0.230	-0.14	4
MoGe	23.930	0.780	0.144	21.309	0.696	0.202	20.851	0.673	0.235	-1.60	7

351 **VLM Spatial Understanding:** Vision-Language Models (VLMs) have demonstrated strong per-
 352 formance in 2D image understanding but remain limited in spatial reasoning Cai et al. (2024).
 353 Since depth maps contain spatial information, incorporating them as additional inputs may improve
 354 VLMs’ 3D understanding. For this proxy task, we adopt SpatialBench Cai et al. (2024) to evaluate
 355 the impact of different depth models on VLM spatial reasoning. We use two VLMs: ChatGPT-4o
 356 and SpatialBot-Phi2-3B Cai et al. (2024). As ChatGPT-4o is not trained with depth, we render
 357 predicted depth maps with the magma colormap and provide paired textual prompts. In contrast,
 358 SpatialBot is jointly trained with paired images and depth maps. Although the released model is
 359 trained with ZoeDepth Bhat et al. (2023), it supports inference with estimated depth from any DFM,
 360 as confirmed in the Official Github Issue #12. We therefore use the official implementation to encode
 361 DFM-predicted depth maps and benchmark all models under the same setup.

363 4 BENCHMARK RESULTS

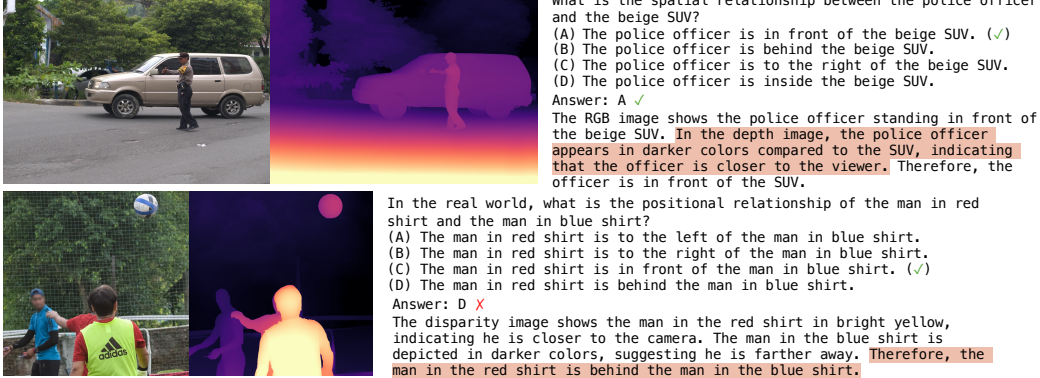
365 **Depth Completion.** Tab. 1 presents the benchmark results. DAV2-Rel Yang et al. (2024b) is the only
 366 method that consistently improves performance across almost all settings, achieving rank 1. Most
 367 methods provide a performance boost, except for Metric3DV2 Hu et al. (2024), which performs
 368 worse than the baseline. Interestingly, depth methods tend to be more beneficial when the available
 369 sparse ground-truth (GT) depth is limited. This suggests that foundation models provide useful
 370 guidance when GT depth is scarce. However, as GT depth increases, the ambiguity in selecting the
 371 appropriate depth source limits further improvements compared to using only sparse GT depth for
 372 guidance. In this case, some DFM even lead to worse performance than the baseline, highlighting
 373 the strong dependence of this task on downstream-compatible DFM.

374 **Stereo Matching.** Tab. 2 presents the results for stereo matching. In the in-domain setting, all
 375 foundation depth models significantly improve baseline performance, with an average 4.5% EPE
 376 gain. However, in zero-shot cross-domain evaluation, not all methods generalize well. DAV2-Rel,
 377 GenPercept Xu et al. (2024), and Marigold Ke et al. (2024) perform best. Metric depth models, such
 378 as Metric3DV2 Hu et al. (2024) and UniDepth Piccinelli et al. (2024), underperform compared to

378 **Table 4: Benchmark with Simultaneous Localization and Mapping (SLAM).** We select Nicer-
 379 SLAM Zhu et al. (2024) as the baseline method and apply depth predictions from various foundation
 380 models as the model input. acc and com are short for accuracy and completion, respectively. Ren-
 381 dered indicates that the input depth map is rendered by the dataset. We exclude Metric3DV2 and
 382 use gray for its results as it is trained with this dataset.

Method	rm-0		rm-1		rm-2		off-0		off-1		off-2		off-3		off-4		imp.	rank
	acc↓	com↓																
w/o depth	3.37	3.93	4.01	4.61	3.58	3.97	7.26	8.25	5.82	6.52	6.98	7.72	6.98	6.92	4.26	6.09	-	-
Midas	3.25	3.63	3.59	4.12	3.49	3.78	8.09	9.04	6.02	7.08	4.63	6.19	4.93	5.40	3.95	5.71	+2.32	5
DAV2-Rel	3.30	3.92	3.52	3.85	3.28	3.59	6.16	6.94	5.78	6.62	6.55	7.09	7.00	6.43	4.26	6.09	+10.00	1
DAV2-Met	3.22	3.39	3.48	3.98	3.47	3.87	8.58	9.64	4.59	5.40	6.38	7.43	6.13	5.59	3.98	6.29	+1.95	6
Metric3DV2	3.48	3.64	3.45	3.93	3.73	4.09	9.55	10.53	5.82	6.41	5.20	6.67	6.73	6.78	4.51	6.65	-4.19	-
UniDepth	3.11	3.49	3.73	4.38	3.80	4.06	5.96	6.91	5.05	6.05	6.48	7.41	5.83	5.95	4.60	6.76	+7.08	2
Marigold	3.01	3.67	3.77	4.07	3.70	4.00	7.07	7.93	6.23	7.01	4.83	6.43	6.32	6.26	4.52	6.79	+4.67	4
GenPercept	3.28	3.47	3.77	4.34	3.33	3.73	7.06	7.65	4.14	5.06	4.38	6.35	5.30	5.05	4.40	6.20	+6.16	3
MoGe	3.26	3.67	3.67	4.23	3.89	4.33	8.86	9.83	4.55	5.58	5.68	6.73	6.40	6.32	3.92	5.98	-4.04	7
Rendered	3.00	3.29	3.69	4.41	4.14	4.47	5.57	6.85	5.95	6.75	5.91	7.91	6.64	6.65	4.01	6.05	-	-

391
 392 **Text Prompt**
 393 We will provide you two images, the first one is the RGB image and the second one is the disparity image. For the
 394 disparity image, we use the magma colormap to render the disparity value. Deeper (farther) areas are depicted in black,
 395 transitioning through purple and pink, to the shallowest (closer) areas in bright yellow. The depth map can be
 396 inaccurate in some areas since it is predicted by a deep learning model. Please ignore this kind of mistake. Your task
 397 is to answer the following question by analyzing the image. Please use the depth map whenever necessary to provide
 398 more accurate and insightful answers.



419 **Figure 3: Showcases of ChatGPT-4o on SpatialBot positional benchmark.** We highlight the
 420 text prompt describing rendered depth map in blue and mistakes made by ChatGPT-4o in red,
 421 respectively. In the first case, ChatGPT-4o correctly answers the question but misinterprets the
 422 depth map despite detailed prompts. As for the second one, despite correctly parsing the depth map,
 423 ChatGPT-4o provides an incorrect answer.

424 other types of depth estimation methods. Notably, DAV2-Met Yang et al. (2024b) outperforms other
 425 metric depth models, possibly benefiting from fine-tuning DAV2-Rel, despite being trained on only
 426 one dataset (Hypersim Roberts et al. (2021)). It somehow aligns with the conclusion in Bhat et al.
 427 (2023). The ability to predict sharper metric depth may also contribute to its superior performance.

428 **Feed-Forward Monocular 3DGs.** Tab. 3 shows the benchmark results. DAV2-Met achieves better
 429 performance compared with DAV2-Rel, suggesting that metric depth properties are beneficial for
 430 novel view synthesis tasks in real 3D environments. MiDaS Ranftl et al. (2022), despite being an
 431 older method, performs remarkably well with a rank of 1. DAV2-Rel also achieves strong results but
 432 slightly underperforms compared to MiDaS. Most metric depth methods, except for DAV2-Met and
 433 affine-invariant depth methods, fail to improve the baseline. Notably, this task exhibits the lowest
 434 correlation with the other proxy tasks, suggesting that it captures a complementary perspective on
 435 DFM quality that is not reflected by the other evaluation metrics.

436 **Simultaneous Localization and Mapping.** Tab. 4 presents the SLAM results. DAV2-Rel achieves
 437 the best results with a promising gap with other methods, indicating a superior potential for this
 438 task. UniDepth achieves the second-best results, highlighting the importance of metric depth for
 439 this task. GenPercept also obtains good results, possibly due to fine-tuning on Hypersim, a sim-
 440 ilar synthetic dataset. Nevertheless, the performance gap between GenPercept and Marigold still

432 **Table 5: Benchmark with spatial understanding of Vision Language Model (VLM).** We evaluate
 433 the effectiveness of depth predictions from various foundation models on the SpatialBench Cai et al.
 434 (2024). The *rank* column is omitted since all depth models perform similarly.

Method	Pos. \uparrow	Exist \uparrow	Count \uparrow	Reach \uparrow	Size \uparrow	Method	Pos. \uparrow	Exist \uparrow	Count \uparrow	Reach \uparrow	Size \uparrow
ChatGPT-4o	64.70	95.00	80.88	54.44	31.11	SpatialBot	61.76	75.00	92.41	51.67	28.33
Midas	62.74	90.00	80.26	54.44	37.22	Midas	55.88	55.00	92.41	46.67	30.00
DAV2-Rel	61.76	88.33	77.11	52.22	35.55	DAV2-Rel	55.88	60.00	93.13	46.67	30.00
DAV2-Met	61.76	86.66	80.44	59.44	38.88	DAV2-Met	55.88	65.00	93.13	45.00	28.33
Metric3DV2	62.74	88.33	79.45	59.44	28.88	Metric3DV2	58.82	55.00	93.13	50.00	28.33
UniDepth	64.70	93.33	80.55	62.22	37.77	UniDepth	58.82	60.00	92.41	53.33	28.33
Marigold	57.84	83.33	80.68	58.88	31.66	Marigold	55.88	60.00	93.13	46.67	30.00
GenPercept	60.78	85.00	81.03	57.77	37.77	GenPercept	55.88	65.00	93.13	48.33	28.33
MoGe	60.78	85.00	79.06	56.11	33.33	MoGe	55.88	60.00	93.13	50.00	28.33

442
 443
 444 highlights the effectiveness of its fine-tuning strategy. Interestingly, we also report results obtained
 445 from the ground-truth depth sensor provided by the dataset, and find that several DFM_s even outper-
 446 form this baseline. This promising result suggests that high-quality DFM_s could serve as effective
 447 alternatives to traditional depth sensors in SLAM applications.

448 **VLM Spatial Understanding.** We use SpatialBench Cai et al. (2024) for this task. Unlike its origi-
 449 nal purpose of benchmarking different vision-language models (VLM_s), we focus on evaluating the
 450 effectiveness of different depth estimations for the same VLM. We select ChatGPT-4o and Spatial-
 451 Bot Cai et al. (2024) as baseline VLM_s, without and with depth inputs during training, respectively.

452 Surprisingly, for both VLM_s, replacing ZoeDepth in SpatialBot with other DFM_s does not signif-
 453 icantly change performance, and ChatGPT-4o also shows little improvement when depth is added.
 454 All DFM_s yield similar results, indicating no clear separation among models for this high-level spa-
 455 tial reasoning task. This saturation likely arises because VLM_s are more sensitive to coarse layout
 456 cues and semantic structure, while being less responsive to fine-grained geometric detail. And most
 457 DFM_s perform similarly well by providing sufficiently accurate coarse structures.

458 For this reason, we exclude VLM spatial understanding from the aggregated results, as it does not
 459 offer meaningful differentiation among DFM_s. Nevertheless, we include qualitative results to high-
 460 light current limitations. Fig. 3 illustrates two examples from the positional benchmark in Spatial-
 461 Bench. In the first, ChatGPT-4o correctly answers the question but misinterprets the depth map
 462 despite detailed prompts, suggesting that training with depth signals is crucial for effective usage. In
 463 the second, ChatGPT-4o parses the depth map correctly but still produces an incorrect answer, under-
 464 scoring the broader limitations of VLM_s in reasoning about 3D space. These findings emphasize
 465 the importance of future research on how VLM_s can better leverage depth beyond coarse structure.

466 **Correlation Analysis.** To further examine the representativeness of BenchDepth, we compute the
 467 Pearson correlation between improvements on our proxy tasks and metrics (delta and AbsRel) from
 468 traditional benchmarks. We use the benchmark from Lotus He et al. (2024) and the VGGT GitHub
 469 Issue #36. We include MiDaS, DAV2-Rel, Metric3DV2, Marigold, GenPercept, and MoGe in this
 470 calculation, as results for DAV2-Met and UniDepth are currently unavailable.

471 As shown in Fig. 1, proxy tasks exhibit strong internal consistency—for example, depth completion
 472 and SLAM show a high correlation of 0.88—suggesting that the selected tasks capture meaningful
 473 shared structure. In contrast, correlations between proxy tasks and traditional benchmarks are weak
 474 or even negative, indicating a clear gap between geometry-centric metrics and downstream utility.
 475 This finding further underscores the importance of BenchDepth as a complementary benchmark for
 476 evaluating DFM_s.

478 5 CONCLUSION

481 We introduced **BenchDepth**, a benchmark for evaluating depth foundation models (DFM_s) through
 482 downstream proxy tasks rather than alignment-based metrics. By benchmarking **eight** SoTA DFM_s
 483 across depth completion, stereo matching, 3D scene reconstruction, SLAM, and vision-language
 484 spatial understanding, we provide a practical assessment of their effectiveness. Our experiments
 485 reveal key insights into the performance improvement of DFM_s in real-world applications. We hope
 BenchDepth can assist the community in selecting DFM_s for downstream applications.

486 REFERENCES
487

488 Josh Achiam, Steven Adler, Sandhini Agarwal, Lama Ahmad, Ilge Akkaya, Florencia Leoni Ale-
489 man, Diogo Almeida, Janko Altenschmidt, Sam Altman, Shyamal Anadkat, et al. Gpt-4 technical
490 report. *arXiv preprint arXiv:2303.08774*, 2023.

491 Shariq Farooq Bhat, Ibraheem Alhashim, and Peter Wonka. Adabins: Depth estimation using adap-
492 tive bins. In *CVPR*, pp. 4009–4018, 2021.

493 Shariq Farooq Bhat, Reiner Birkl, Diana Wofk, Peter Wonka, and Matthias Müller. Zoedepth: Zero-
494 shot transfer by combining relative and metric depth. *arXiv preprint arXiv:2302.12288*, 2023.

495

496 Wenxiao Cai, Iaroslav Ponomarenko, Jianhao Yuan, Xiaoqi Li, Wankou Yang, Hao Dong, and
497 Bo Zhao. Spatialbot: Precise spatial understanding with vision language models. *arXiv preprint*
498 *arXiv:2406.13642*, 2024.

499 Weifeng Chen, Zhao Fu, Dawei Yang, and Jia Deng. Single-image depth perception in the wild.
500 *NeurIPS*, 29, 2016.

501

502 Junda Cheng, Longliang Liu, Gangwei Xu, Xianqi Wang, Zhaoxing Zhang, Yong Deng, Jinliang
503 Zang, Yurui Chen, Zhipeng Cai, and Xin Yang. Monster: Marry monodepth to stereo unleashes
504 power. *arXiv preprint arXiv:2501.08643*, 2025.

505 Wenyang Cong, Yiqing Liang, Yancheng Zhang, Ziyi Yang, Yan Wang, Boris Ivanovic, Marco
506 Pavone, Chen Chen, Zhangyang Wang, and Zhiwen Fan. E3d-bench: A benchmark for end-
507 to-end 3d geometric foundation models. *arXiv preprint arXiv:2506.01933*, 2025.

508

509 Marius Cordts, Mohamed Omran, Sebastian Ramos, Timo Rehfeld, Markus Enzweiler, Rodrigo
510 Benenson, Uwe Franke, Stefan Roth, and Bernt Schiele. The cityscapes dataset for semantic
511 urban scene understanding. In *CVPR*, pp. 3213–3223, 2016.

512 David Eigen, Christian Puhrsch, and Rob Fergus. Depth map prediction from a single image using
513 a multi-scale deep network. *NeurIPS*, 27, 2014.

514 Huan Fu, Mingming Gong, Chaohui Wang, Kayhan Batmanghelich, and Dacheng Tao. Deep ordinal
515 regression network for monocular depth estimation. In *CVPR*, pp. 2002–2011, 2018.

516

517 Gonzalo Martin Garcia, Karim Abou Zeid, Christian Schmidt, Daan de Geus, Alexander Hermans,
518 and Bastian Leibe. Fine-tuning image-conditional diffusion models is easier than you think. *arXiv*
519 *preprint arXiv:2409.11355*, 2024.

520

521 Yongtao Ge, Guangkai Xu, Zhiyue Zhao, Libo Sun, Zheng Huang, Yanlong Sun, Hao Chen, and
522 Chunhua Shen. Geobench: Benchmarking and analyzing monocular geometry estimation models.
523 *arXiv preprint arXiv:2406.12671*, 2024.

524

525 Andreas Geiger, Philip Lenz, and Raquel Urtasun. Are we ready for autonomous driving? the kitti
526 vision benchmark suite. In *CVPR*, pp. 3354–3361. IEEE, 2012.

527

528 Andreas Geiger, Philip Lenz, Christoph Stiller, and Raquel Urtasun. Vision meets robotics: The
529 kitti dataset. *The international journal of robotics research*, 32(11):1231–1237, 2013.

530

531 Jing He, Haodong Li, Wei Yin, Yixin Liang, Leheng Li, Kaiqiang Zhou, Hongbo Zhang, Bingbing
532 Liu, and Ying-Cong Chen. Lotus: Diffusion-based visual foundation model for high-quality dense
533 prediction. *arXiv preprint arXiv:2409.18124*, 2024.

534

535 Kaiming He, Haoqi Fan, Yuxin Wu, Saining Xie, and Ross Girshick. Momentum contrast for
536 unsupervised visual representation learning. In *CVPR*, pp. 9729–9738, 2020.

537

538 Mu Hu, Wei Yin, Chi Zhang, Zhipeng Cai, Xiaoxiao Long, Hao Chen, Kaixuan Wang, Gang Yu,
539 Chunhua Shen, and Shaojie Shen. Metric3d v2: A versatile monocular geometric foundation
540 model for zero-shot metric depth and surface normal estimation. *IEEE TPAMI*, 2024.

541

542 Hualie Jiang, Zhiqiang Lou, Laiyan Ding, Rui Xu, Minglang Tan, Wenjie Jiang, and Rui Huang.
543 Defom-stereo: Depth foundation model based stereo matching. *arXiv preprint arXiv:2501.09466*,
544 2025.

540 Jared Kaplan, Sam McCandlish, Tom Henighan, Tom B Brown, Benjamin Chess, Rewon Child,
 541 Scott Gray, Alec Radford, Jeffrey Wu, and Dario Amodei. Scaling laws for neural language
 542 models. *arXiv preprint arXiv:2001.08361*, 2020.

543

544 Bingxin Ke, Anton Obukhov, Shengyu Huang, Nando Metzger, Rodrigo Caye Daudt, and Konrad
 545 Schindler. Repurposing diffusion-based image generators for monocular depth estimation. In
 546 *CVPR*, pp. 9492–9502, 2024.

547

548 Bernhard Kerbl, Georgios Kopanas, Thomas Leimkühler, and George Drettakis. 3d gaussian splat-
 549 ting for real-time radiance field rendering. *ACM Trans. Graph.*, 42(4):139–1, 2023.

550

551 Junnan Li, Dongxu Li, Silvio Savarese, and Steven Hoi. Blip-2: Bootstrapping language-image
 552 pre-training with frozen image encoders and large language models. In *International conference
 553 on machine learning*, pp. 19730–19742. PMLR, 2023a.

554

555 Yinhao Li, Zheng Ge, Guanyi Yu, Jinrong Yang, Zengran Wang, Yukang Shi, Jianjian Sun, and
 556 Zeming Li. Bevdepth: Acquisition of reliable depth for multi-view 3d object detection. In *AAAI*,
 557 volume 37, pp. 1477–1485, 2023b.

558

559 Zhenyu Li, Xuyang Wang, Xianming Liu, and Junjun Jiang. Binsformer: Revisiting adaptive bins
 560 for monocular depth estimation. *arXiv preprint arXiv:2204.00987*, 2022.

561

562 Zhenyu Li, Shariq Farooq Bhat, and Peter Wonka. Patchfusion: An end-to-end tile-based framework
 563 for high-resolution monocular metric depth estimation. *arXiv preprint arXiv:2312.02284*, 2023c.

564

565 Zhenyu Li, Zehui Chen, Xianming Liu, and Junjun Jiang. Depthformer: Exploiting long-range
 566 correlation and local information for accurate monocular depth estimation. *Machine Intelligence
 567 Research*, pp. 1–18, 2023d.

568

569 Zhenyu Li, Shariq Farooq Bhat, and Peter Wonka. Patchrefiner: Leveraging synthetic data for real-
 570 domain high-resolution monocular metric depth estimation. *arXiv preprint arXiv:2406.06679*,
 571 2024.

572

573 Nikolaus Mayer, Eddy Ilg, Philip Hausser, Philipp Fischer, Daniel Cremers, Alexey Dosovitskiy,
 574 and Thomas Brox. A large dataset to train convolutional networks for disparity, optical flow, and
 575 scene flow estimation. In *CVPR*, pp. 4040–4048, 2016.

576

577 Maxime Oquab, Timothée Darcet, Théo Moutakanni, Huy Vo, Marc Szafraniec, Vasil Khalidov,
 578 Pierre Fernandez, Daniel Haziza, Francisco Massa, Alaaeldin El-Nouby, et al. Dinov2: Learning
 579 robust visual features without supervision. *arXiv preprint arXiv:2304.07193*, 2023.

580

581 Jin-Hwi Park, Chanhwi Jeong, Junoh Lee, and Hae-Gon Jeon. Depth prompting for sensor-agnostic
 582 depth estimation. In *CVPR*, pp. 9859–9869, 2024.

583

584 Luigi Piccinelli, Yung-Hsu Yang, Christos Sakaridis, Mattia Segu, Siyuan Li, Luc Van Gool, and
 585 Fisher Yu. Unidepth: Universal monocular metric depth estimation. In *CVPR*, pp. 10106–10116,
 586 2024.

587

588 René Ranftl, Katrin Lasinger, David Hafner, Konrad Schindler, and Vladlen Koltun. Towards robust
 589 monocular depth estimation: Mixing datasets for zero-shot cross-dataset transfer. *IEEE TPAMI*,
 44(3), 2022.

590

591 Mike Roberts, Jason Ramapuram, Anurag Ranjan, Atulit Kumar, Miguel Angel Bautista, Nathan
 592 Paczan, Russ Webb, and Joshua M Susskind. Hypersim: A photorealistic synthetic dataset for
 593 holistic indoor scene understanding. In *ICCV*, pp. 10912–10922, 2021.

594

595 Robin Rombach, Andreas Blattmann, Dominik Lorenz, Patrick Esser, and Björn Ommer. High-
 596 resolution image synthesis with latent diffusion models. In *CVPR*, pp. 10684–10695, 2022.

597

598 Olaf Ronneberger, Philipp Fischer, and Thomas Brox. U-net: Convolutional networks for biomedical
 599 image segmentation, 2015.

594 Daniel Scharstein, Heiko Hirschmüller, York Kitajima, Greg Krathwohl, Nera Nešić, Xi Wang, and
 595 Porter Westling. High-resolution stereo datasets with subpixel-accurate ground truth. In *Pattern*
 596 *Recognition: 36th German Conference, GCPR 2014, Münster, Germany, September 2-5, 2014, Proceedings 36*, pp. 31–42. Springer, 2014.

598 Thomas Schops, Johannes L Schonberger, Silvano Galliani, Torsten Sattler, Konrad Schindler, Marc
 599 Pollefeys, and Andreas Geiger. A multi-view stereo benchmark with high-resolution images and
 600 multi-camera videos. In *CVPR*, pp. 3260–3269, 2017.

602 Nathan Silberman, Derek Hoiem, Pushmeet Kohli, and Rob Fergus. Indoor segmentation and sup-
 603 port inference from rgbd images. In *ECCV*, pp. 746–760. Springer, 2012.

604 Oriane Siméoni, Huy V Vo, Maximilian Seitzer, Federico Baldassarre, Maxime Oquab, Cijo Jose,
 605 Vasil Khalidov, Marc Szafraniec, Seungeun Yi, Michaël Ramamonjisoa, et al. Dinov3. *arXiv*
 606 *preprint arXiv:2508.10104*, 2025.

607 Julian Straub, Thomas Whelan, Lingni Ma, Yufan Chen, Erik Wijmans, Simon Green, Jakob J Engel,
 608 Raul Mur-Artal, Carl Ren, Shobhit Verma, et al. The replica dataset: A digital replica of indoor
 609 spaces. *arXiv preprint arXiv:1906.05797*, 2019.

611 Stanislaw Szymanowicz, Eldar Insafutdinov, Chuanxia Zheng, Dylan Campbell, Joao F Henriques,
 612 Christian Rupprecht, and Andrea Vedaldi. Flash3d: Feed-forward generalisable 3d scene recon-
 613 struction from a single image. *arXiv preprint arXiv:2406.04343*, 2024.

614 Jianyuan Wang, Minghao Chen, Nikita Karaev, Andrea Vedaldi, Christian Rupprecht, and David
 615 Novotny. Vggt: Visual geometry grounded transformer. In *CVPR*, pp. 5294–5306, 2025.

617 Ruicheng Wang, Sicheng Xu, Cassie Dai, Jianfeng Xiang, Yu Deng, Xin Tong, and Jiaolong Yang.
 618 Moge: Unlocking accurate monocular geometry estimation for open-domain images with optimal
 619 training supervision. *arXiv preprint arXiv:2410.19115*, 2024a.

621 Shuzhe Wang, Vincent Leroy, Yohann Cabon, Boris Chidlovskii, and Jerome Revaud. Dust3r: Ge-
 622 ometric 3d vision made easy. In *CVPR*, pp. 20697–20709, 2024b.

623 Bowen Wen, Matthew Trepte, Joseph Aribido, Jan Kautz, Orazio Gallo, and Stan Birchfield. Foun-
 624 dationstereo: Zero-shot stereo matching. In *CVPR*, pp. 5249–5260, 2025.

626 Gangwei Xu, Xianqi Wang, Xiaohuan Ding, and Xin Yang. Iterative geometry encoding volume for
 627 stereo matching. In *CVPR*, pp. 21919–21928, 2023.

628 Guangkai Xu, Yongtao Ge, Mingyu Liu, Chengxiang Fan, Kangyang Xie, Zhiyue Zhao, Hao Chen,
 629 and Chunhua Shen. What matters when repurposing diffusion models for general dense percep-
 630 tion tasks? *arXiv preprint arXiv:2403.06090*, 2024.

632 Lihe Yang, Bingyi Kang, Zilong Huang, Xiaogang Xu, Jiashi Feng, and Hengshuang Zhao. Depth
 633 anything: Unleashing the power of large-scale unlabeled data. *arXiv preprint arXiv:2401.10891*,
 634 2024a.

635 Lihe Yang, Bingyi Kang, Zilong Huang, Zhen Zhao, Xiaogang Xu, Jiashi Feng, and Hengshuang
 636 Zhao. Depth anything v2. *arXiv preprint arXiv:2406.09414*, 2024b.

638 Lvmin Zhang, Anyi Rao, and Maneesh Agrawala. Adding conditional control to text-to-image
 639 diffusion models. In *ICCV*, pp. 3836–3847, 2023.

640 Tinghui Zhou, Richard Tucker, John Flynn, Graham Fyffe, and Noah Snavely. Stereo magnification:
 641 Learning view synthesis using multiplane images. *arXiv preprint arXiv:1805.09817*, 2018.

642

643 Zihan Zhu, Songyou Peng, Viktor Larsson, Zhaopeng Cui, Martin R Oswald, Andreas Geiger, and
 644 Marc Pollefeys. Nicer-slam: Neural implicit scene encoding for rgbd slam. In *2024 International*
 645 *Conference on 3D Vision (3DV)*, pp. 42–52. IEEE, 2024.

646 Yiming Zuo, Karhan Kayan, Maggie Wang, Kevin Jeon, Jia Deng, and Thomas L Griffiths. Towards
 647 foundation models for 3d vision: How close are we? *arXiv preprint arXiv:2410.10799*, 2024.

648 **A LARGE LANGUAGE MODELS USAGE**
649

650 We used ChatGPT to polish the paper.
651

652

653

654

655

656

657

658

659

660

661

662

663

664

665

666

667

668

669

670

671

672

673

674

675

676

677

678

679

680

681

682

683

684

685

686

687

688

689

690

691

692

693

694

695

696

697

698

699

700

701